CASMO-5 energy release per fission model

[*]Joel Rhodes[a], Kord Smith[a], and Zhiwen Xu[a,]

[a] Studsvik Scandpower Inc., Idaho Falls, USA

Abstract

This paper details the energy release model implemented in Studsvik's CASMO-5 lattice physics code. By utilizing internally computed neutron capture rates, the capture component of the total recoverable energy is more accurately calculated, and the use of traditionally assumed constant values of energy release per capture (employed in most lattice physics codes) has been eliminated. By using problem-specific capture rates in the energy release model, the impacts of depletion, gadolinia, boron concentrations, MOX compositions, and void fraction are naturally incorporated into the energy release calculation. CASMO-5 studies performed with ENDF/B-VII data show that the traditional capture energy release values for standard LWR applications are too large. Also, the implications for energy release in downstream 3-D reactor simulator codes are discussed.

1. Introduction

During the development of Studsvik's next generation lattice physics code, CASMO-5 (Rhodes, et al., 2006), all constituent physics models have been scrutinized to identify approximations that could be eliminated or improved. Since one of the most important parameters predicted by lattice physics codes is the reactivity changes with fuel depletion, computed results are sensitive to the assumed amount of energy released per fission event. Recent work (Madland, 2006) and updated data in ENDF/B-VII data files provides extensive measured data and correlations for the isotopic dependence of the <u>direct</u> energy release per fission.

Reactor analysis, however, also requires accurate knowledge of <u>indirect</u> energy released from parasitic capture of neutrons and decay of transmuted nuclides. The energy released from neutron captures is not only a function of the fissioning isotope, but also a complex function of the location and process (e.g., both in spatial location and by capturing nuclide) by which neutrons are ultimately captured. However, lattice physics codes have historically modeled capture energy release as simple constants, determined from calculations of generic reactors and materials. Such capture rate calculations have been used to deduce suitable average values of energy release, and typical values referenced in the literature are 6.1 (James, 1969, James, 1971, Pêrsîc and Trkov, 1999) or 5.991 (Tasaka, 1990) MeV/capture - independent of the lattice composition.

Our review of the widely referenced historical publications determined that errors have been made in the computation of the average values of energy released per capture. For example, the reference value of 6.1 MeV/capture ignored all captures outside the fuel. Since as much as 10% of neutron captures in LWR lattices can occur in coolant hydrogen (with an energy release of only 2.22 MeV/capture), there was concern that the value of 6.1 MeV/capture is too large. The reference value of 5.991 MeV/capture was calculated with an incorrectly assigned value of 6.25 MeV (the value for deuterium) rather than the correct 2.22 MeV per hydrogen capture. Such oversights led to a decision to abandon the historically referenced capture data and introduce upgraded methods to compute the capture energy release directly in CASMO-5.

---

[*] Corresponding author, joel.rhodes@studsvik.com

Tel: +1 (208) 522-1060; Fax: +1 (208) 522-1187

This paper details the resulting upgraded energy release model of CASMO-5.

2. Approach

The CASMO-5 lattice physics code provides detailed capture and fission rates for every nuclide, in each spatial region, at each depletion point. Consequently, there is no intrinsic reason for energy release per capture to be approximated by generic constants. Rather, the energy released per capture can be directly computed from detailed capture rates - providing a lattice-dependent and depletion-dependent model for the energy release per capture.

The fission energy release model is not required by the neutronics solution. However, it is a key component in depletion calculations since this model determines the burnup rate. The CASMO-5 depletion methodology employs a standard predictor/corrector isotope depletion model and the lattice power density is assumed to be constant over a depletion step. The constant power density assumption (as opposed to a constant flux approximation) requires an iterative determination of the depletion time step (in seconds) to achieve a desired depletion step (in MWd/kg). For purposes of this iterative process, it is still desirable to convert energy releases per fission and per capture to a constant value of total energy release per fission, but the values need only be assumed fixed for a single depletion step. This approach leads to a natural iterative determination of the energy release per capture as a function of the depleted fuel composition (including MOX composition) and lattice type.

3. Background

The direct energy release per fission includes: kinetic energy of fission fragments, kinetic energy of prompt fission neutrons, kinetic energy of delayed fission neutrons, total energy of the prompt gammas, total energy of the delayed gammas, energy released by delayed betas, and energy carried away by anti-neutrinos. This direct energy release per fission of isotope i is approximated in ENDF/B-VII by excluding the kinetic energy of incident neutrons (E) and the energy of anti-neutrinos by the empirical expression (Oblozinsky and Herman, 2006):

$$ER_i(E) = ER_i(0) + 1.157E - 8.07 [\nu_i(E) - \nu_i(0)] \quad (1)$$

An additional term which accounts for the indirect energy from capture gammas and decay energy of capture products must be added to Eq.1, and it is typically approximated by:

$$EC_i = [\nu_i(E) - 1] \overline{Q}_c \quad (2)$$

where $\overline{Q}_c$ is typically 6.1 MeV or 5.991 MeV. CASMO-4 (Knott et al., 1995) and HELIOS (Studsvik Scandpower, 1998) use 5.991 MeV/capture, and WIMS-D (Aldama et al.., 2003) uses 6.1 MeV/capture.

Consequently, the total energy release per fission for fissionable isotope i (in MeV) is then given by:

$$\kappa_i(E) = ER_i(0) + 1.157E - 8.07 [\nu_i(E) - \nu_i(0)] + [\nu_i(E) - 1] \overline{Q}_{c,} \quad (3)$$

where $ER_i(0)$ and $\nu_i(0)$ are taken directly from ENDF/B-VII files: MF=1; MT=458 and MT=452, respectively.

4. CASMO-5 Implementation

The integral of Eq. 3 is approximated in CASMO-5 by:

$$\kappa_i \approx ER_i(0) + 1.157 \overline{E}_i - 8.07 [\overline{V}_i - \nu_i(0)] + [\overline{V} - 1] \overline{Q}_c \quad (4)$$

where the mean fissioning neutron energy for isotope i is defined directly from the 586 group cross sections and fluxes (and ignoring spatial dependence for simplification here) as:

$$\overline{E}_i \equiv \frac{\sum_g E_{ave,g} \sigma_{f,g,i} \phi_g}{\sum_g \sigma_{f,g,i} \phi_g}, \quad (5)$$

where $E_{ave,g}$ is the average group energy, $\sigma_{f,g,i}$ is the fission cross section for isotope i in group g and ϕ_g is the neutron flux. Mean values of the number of neutrons emitted per fission are defined as:

$$\overline{V}_i \equiv \frac{\sum_g \nu_{g,i} \sigma_{f,g,i} \phi_g}{\sum_g \sigma_{f,g,i} \phi_g} \quad (6)$$

and

$$\overline{V} \equiv \frac{\sum_i n_i \sum_g \nu_{g,i} \sigma_{f,g,i} \phi_g}{\sum_i n_i \sum_g \sigma_{f,g,i} \phi_g}. \quad (7)$$

The mean energy released per capture, $\overline{Q}_c$, is then defined as:

$$\overline{Q}_c \equiv \frac{\sum_i q_i n_i \sum_g \sigma_{c,g,i} \phi_g}{\sum_i n_i \sum_g \sigma_{c,g,i} \phi_g}, \qquad (8)$$

where n_i is the number density of isotope i, and the summation is over all nuclides. The q_i's are the recoverable energy per capture (including subsequent short-term decay) and some important values are displayed in Table 1 (CASMO-5 actually tabulates q_i data for 46 heavy nuclides and 84 fission products/structural materials). CASMO-5 uses Eqs (4) to (8) to compute problem-specific values of $\overline{Q}_c$ and κ_i "on-the-fly." The modeling of direct energy release for different isotopes has been well addressed by traditional models. The new CASMO-5 model improves the computation of the indirect neutron capture contributions.

Table 1
Neutron capture energies (q_i) for typical LWR isotopes.

Isotope	q_i (MeV)	Isotope	q_i(MeV)
H-1	2.2246	Mo-95	9.1543
H-2	6.2570	Tc-99	8.1615 (1)
B-10	2.7895	Rh-103	7.9964
O-16	4.1434	Rh-105	8.2042 (1)
U-234	5.2978	Xe-131	8.9350
U-235	6.5452	Xe-135	7.9904
U-238	5.6784	Nd-143	7.8160
Pu-239	6.5337	Nd-145	7.5650
Pu-240	5.2410	Sm-150	5.5965
Pu-241	6.3008	Sm-151	8.2580
Pu-242	5.2658 (1)	Gd-155	8.5364
Am-243	6.4716 (1)	Gd-157	7.9374

(1) Includes one beta decay

The low q_i values for H-1 and B-10 ((n,α) rather than capture) in coolant and moderator are very important because their large capture fractions significantly reduce $\overline{Q}_c$.

5.   Results from CASMO-5 Calculations

Mean capture energies calculated by CASMO-5 and those reported by James and by Pêrsîc are compared in Table 2, for two modern LWR fuel assemblies:

- 17x17 PWR lattice, 4.5 wt% U-235, Gd free, at 0 and 800 ppm boron
- 10x10 BWR lattice, 4.6 wt% U-235 (with 17 pins of 7 wt% gadolinia) at 0% and 80 % void

The two depletion shapes of $\overline{Q}_c$ displayed in Fig. 1 (PWR at 800 ppm and BWR at 0% void), together with isotopic q_i data from Table 1, leads to several key observations.

First, for PWR lattices, both the James and Pêrsîc $\overline{Q}_c$ values are too high. This results from neglecting hydrogen and boron (and other materials outside the fuel) when calculating $\overline{Q}_c$. Table 2 also displays CASMO-5 results computed by ignoring hydrogen in the calculation of $\overline{Q}_c$ (labeled no H), and these results are much closer to both James and Pêrsîc (as expected). Differences are further exacerbated for higher boron concentrations, as significantly more captures occur in B-10.

Secondly, one expects $\overline{Q}_c$ to increase with depletion, as the high q_i values for fission products become larger contributors. The expected increase is observed in the PWR lattice (Gd free). However, for the heavily Gd-loaded BWR, the $\overline{Q}_c$ behavior with depletion is much different. Early on, it is dominated by the high q_i values of Gd-155 and Gd-157 (8.5 and 7.9 MeV/capture respectively). As the Gd burns away, $\overline{Q}_c$, decreases, and ultimately the curve joins the Gd free PWR curve. The net impact on reactivity can be as large as +/- 70 pcm over the course of a depletion.
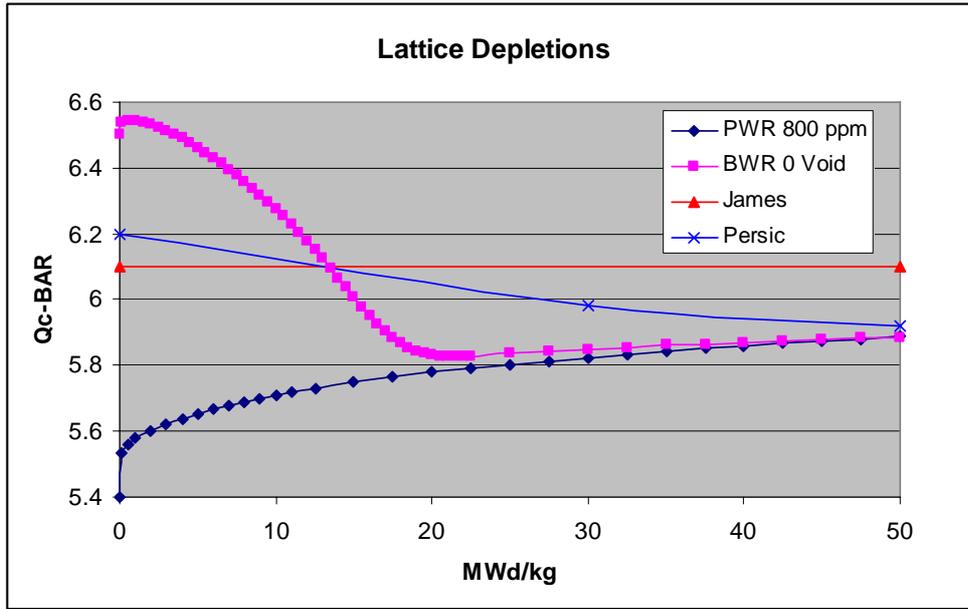
Fig. 1. CASMO-5 calculation of $\overline{Q}_c$ with depletion.

Table 2

CASMO-5 $\overline{Q}_c$ for PWR and BWR lattices.

	$\overline{Q}_c$ (MeV/capture)	
	0.0 MWd/kg	50 MWd/kg
James	6.1+/- 0.3	6.1 +/- 0.3
Pêrsîc (PWR)	6.20	5.92
PWR BOR = 0 ppm	5.70	6.10
PWR BOR = 800 ppm	5.40	5.89
PWR BOR = 0 ppm (no H)	6.02	6.30
PWR BOR = 800 ppm (no H)	5.64	6.05
BWR Void = 0 %	6.50	5.89
BWR Void = 80 %	6.57	6.12
BWR Void = 0% (no H)	6.94	6.35
BWR Void = 80 % (no H)	6.80	6.32

6. Spatial Variations in Capture Energy

The data presented in previous sections details the variations in average energy released per capture that occur because of fuel assembly materials and/or fission product generation. There also exists a more subtle (and often more important) variation in the neutron capture energies that arises because neutrons may be captured in a fuel assembly other than the one in which the fission neutrons are released.

The capture energy term in Eq. 4, $[\overline{\nu} - 1]\overline{Q}_c$, arises from the assumption that all fission and captures occur in a critical reactor system (e.g., k-eff = 1.000). Thus, the $\overline{\nu} - 1$ excess neutrons that leak from an assembly are assumed to be captured in an identical assembly. In most power producing reactors, some fuel assemblies have k-infinities greater that one (e.g., fresh fuel) and others have k-infinities less than one (e.g., depleted fuel, assemblies with burnable absorbers, etc). Consequently, the high reactivity fuel assemblies actually contribute their excess neutrons to increasing the captures in low reactivity assemblies.

There are several ways that this spatial redistribution of energy could be handled in 3-D reactor analysis codes (e.g., nodal codes such as SIMULATE-4 (Bahadir et al., 2005)) downstream from the lattice physics code. One straightforward approach would be to track the individual isotopic fission and capture rates in the 3-D simulator and use single-assembly-generated isotopic fission and capture energies as tabulated in CASMO-5. This approach would involve little additional approximation, but would require an extensive tracking of isotopic number densities in the 3-D simulators and the transfer of a large quantity of energy production data from CASMO-5.

The traditional approach used in 3-D nodal simulators is to simply average all isotopic fission and capture energies from single-assembly lattice calculations to obtain an average energy released per

4

fission - which is tabulated versus burnup and history variables used in the 3-D simulator. Data generated with CASMO-5 for four BOL PWR assemblies are presented in Table 3. From the data presented in the first half of this table, one can observe that the direct energy produced per fission has little variation with assembly enrichment or Gd absorbers. The energy release per neutron capture has little enrichment variation, but is sensitive to the Gd captures, as mentioned in previous sections of this paper.

The real question, however, is how much energy is released in each bundle when the reactor core contains many different types of fuel assemblies. To explore such situations, two different two-assembly problems were computed with CASMO-5. Problem #1 is a core containing one 0.70 w% U-235 assembly and another 1.33 w% U-235 assembly. Problem #2 is a core containing one 2.44 w% U-235 assembly and another 2.44 w% U-235 assembly with many Gd-bearing pins. Both configurations were chosen so that the simulated "reactor" was critical. The second half of Table 3 details results for each of the fuel assemblies in the two-assembly cores. By comparing results from the two-assembly cores with the single-assembly results, one observes the following:

1. The direct energy produced per fission in each assembly type is essentially the same in the reactor and single-assembly.

2. The direct energy produced per capture in each assembly type is essentially the same in the reactor and single-assembly.

3. The number of excess neutrons ($\overline{\nu} - 1$) produced in each assembly type is essentially the same in the reactor and single-assembly.

4. The mean number of neutrons per fission minus 1.0 is a poor estimate of the actual capture-to-fission ratios.

The good agreement between the single-assembly and reactor values for the first three quantities indicates that the spectrum in the single-assembly calculation is quite close to that of the same assembly in a critical reactor. The poor agreement between nu-bar minus one and the capture-to-fission ratio arises because the k-infinity of the fuel assemblies are not unity, and the high reactivity assemblies actually contribute neutrons to the capture in the lower reactivity assemblies in the reactor.

However, if the capture-to-fission ratios from the single-assemblies are compared with those of the reactor configuration, there is quite good agreement. In fact, if the definition of the total energy produced

per fission (Eq. 4) is changed from using $\overline{\nu} - 1$ to using the single-assembly capture-to-fission ratio, an excellent prediction of the energy released per fission in each assembly type of the reactor geometry is obtained. This implies that the effect of maintaining criticality in the single-assembly calculation by introducing k-eff (to maintain criticality) closely approximates the actual effect of inter-assembly leakage in the core geometries (at least with respect to energy released from fission and captures).

The results of the direct CASMO-5 BOL core calculations displayed in Table 3 demonstrate that total energy released per fission is 1% higher in the low enriched and 1% lower in the high enrichment assemblies than traditionally modeled. Similarly in low reactivity Gd assemblies, the total energy released per fission can be 5% higher energy than traditionally modeled.

Altering the traditional definition of energy yields per fission for use in a 3-D nodal simulator will give rise to two principal changes. The first change is that the distribution of thermal energy transferred from the neutronics to the thermal hydraulics will be altered to reflect more accurately the location of neutron capture energy production. Clearly, a definition of capture energy that uses the single-assembly capture-to-fission rates results in a more accurate reactor distribution of thermal energy.

The second change in the 3-D simulation will be an alteration of the relationship between time and energy production used in the solution of isotopic depletion equations. For the two examples presented here, we can assess the changes in the relationship between total energy production and total fission rate, which are displayed in Table 4 (where it has been assumed that the 3-D simulator predicts exactly the node-wise capture-to-fission ratios). As expected, using the capture energy definition with the capture-to-fission ratios from the single-assembly calculation leads to a more accurate prediction than the $\overline{\nu} - 1$ approximation, but the overall differences are small. This is expected, since the reactor-averaged fission-to-energy conversion is not sensitive to where the capture energy is produced, but only that the energy is produced somewhere.

These results demonstrate that changing the definitions of total energy produced per fission to reflect a more accurate approximation of the capture-to-fission ratios is advantageous if the nodal simulators treat the fission-to-energy conversion with a single conversion as computed by a lattice physics code. On the other hand, if both the direct and capture energy conversion data are transferred from the lattice physics code to the 3-D nodal simulator, the total energy could be reconstructed even more accurately using the simulator values of node-wise capture-to-fission ratios.

5

Table 3
Energy Release per Fission for Various PWR Fuel Assemblies

	Single-Assembly Calculations with Reflective Boundaries			
Fuel Assembly	**0.70 w%**	**1.33 w%**	**2.44 w%**	**2.44w%+Gd**
k-infinity	0.874	1.100	1.271	0.638
$\overline{\nu}$	2.468	2.462	2.459	2.481
Q_{direct} (MeV/fission)	193.88	193.80	193.75	194.01
Q_c (MeV/capture)	5.24	5.39	5.57	6.89
$\overline{\nu}$ -1	1.468	1.462	1.459	1.482
Capture/Fission Rate	1.837	1.245	0.940	2.900
Q_{total} * (MeV/fission)	201.58	201.68	201.86	204.21
Q_{total} **(MeV/fission)	203.48	200.51	198.98	213.99

	Two-Assembly Calculations with Reflective Boundaries			
	Problem # 1 **enrichment variation**		**Problem # 2** **with/without Gd**	
Fuel Assembly	**0.70 w%**	**1.33 w%**	**2.44 w%**	**2.44w%+Gd**
Fission Production Rate	0.775	1.227	1.455	0.549
Capture Rate	0.583	0.614	0.568	0.629
k-infinity	0.867	1.107	1.259	0.647
$\overline{\nu}$	2.468	2.462	2.462	2.472
Q_{direct} (MeV/ fission)	193.88	193.80	193.79	193.93
Q_c (MeV/capture)	5.25	5.39	5.56	6.90
$\overline{\nu} - 1$	1.468	1.462	1.462	1.472
Capture/Fission Rate	1.855	1.232	0.959	2.833
Q_{total} ** (MeV/fission)	203.61	200.44	199.14	213.46

* $Q_{total} = Q_{direct} + (\overline{\nu} - 1)$ x $Q_{capture}$
** $Q_{total} = Q_{direct} + $ (capture rate/fission rate) x $Q_{capture}$

Table 4
Average Reactor Energy Released (MeV/fission)

	Single-Assembly Data		Ref. Solution
	$\overline{\nu} - 1$	Capture/Fission	
Problem #1	201.64	201.66	201.67
Problem #2	202.50	203.08	203.05

7. Other Spatial Approximations

The direct energy production as a result of fission as defined by Madland and incorporated in ENDF data definitions includes all energy from prompt and delayed gammas, as well as the energy of fission neutrons. In the analysis of Section 6, all of the direct energy from fission was assumed to be absorbed in the fuel assembly in which the fission occurs. Clearly, this is not rigorous, since neutrons and gammas produced in high power assemblies actually deposit some their energy in other fuel assemblies. To treat this phenomenon exactly, one should compute coupled neutron-photon calculations for the exact reactor geometry and tabulate the locations at which all particle energies are deposited. At present, this is beyond the capability of modern 3-D nodal reactor simulators, and these effects have been ignored here.

8. Conclusions

Pêrsîc's conclusion that James' assertion that a value of 6.1+/- 0.3 MeV/capture may be reliably used for a wide range of thermal reactors is only valid to within approximately +/-0.7 MeV.

From CASMO-5 calculations, the values of 6.1 (and 5.991) MeV/capture appear to be too high to be representative of LWRs at most reactor conditions. The first value resulted from neglecting capture in low q_i materials like H-1 and B-10, and the second value (from JAERI-1320) is apparently simply a mistake (using the q_i value of H-2 for H-1). Both of these values are widely used within the industry.

CASMO-5 results show that there exist clear dependencies of LWR capture energy yields on fuel exposure, Gd and boron concentrations, MOX compositions, and void fractions. The use of fixed values clearly misses important features that impact reactor depletion results.

The CASMO-5 energy release per fission model takes advantage of the latest data (ENDF/B-VII R0) and detailed problem-specific capture and fission rates to compute accurately the isotopic energy yields as lattice compositions evolve.

References

Aldama, D., Leszczynski, F., and Trkov, A., 2003. "WIMS-D Library Update Project," Coordinated Research Project Final Report, IAEA, Vienna.

Bahadir T., Lindahl, S-Ö, Palmtag, S.P., 2005. "SIMULATE-4 Multi-group Nodal Code with Microscopic Depletion Model," ANS Topical Meeting in Mathematical Computations, Avignon, France.

"HELIOS Methods," in Program Manual Rev. 3, Program HELIOS-1.5, 1998. Studsvik Scandpower, Inc.

James, M., 1969. "Energy Released in Fission," Journal of Nuclear Energy, Vol. 23, Pergamon Press, Ireland, pp 517 to 536.

James, M, 1971. "The Useful Energy Released in the Fission of ^{232}Th, ^{233}U, ^{234}U, ^{236}U, ^{237}Np, ^{238}Pu, ^{240}Pu, and ^{242}Pu," Journal of Nuclear Energy, Vol. 25, Pergamon Press, Ireland, pp 513 to 523.

Knott, D., et al., 1995. "CASMO-4 Methodology Manual," Studsvik/SOA-95/02, Studsvik of America, Inc.

Madland, D., 2006. "Total Prompt Energy Release in the Neutron Induced Fission of ^{235}U, ^{238}U, and ^{239}Pu," Nucl. Phys., Vol. A772, p 113.

Oblozinsky, P., and Herman, M., 2006. "Special Issue on Evaluated Nuclear Data File ENDF/B-VII.0," Nuclear Data Sheets, Volume 107, Number 12.

Pêrsîc, A. and Trkov, A., 1999. "The Energy Released by Neutron Capture in Thermal Reactors," International Conference Nuclear Energy in Central Europe '99, Portotoz, Slovenia.

Rhodes, J., Smith, K.S., and Lee, D., 2006. "CASMO-5 Development and Applications," PHYSOR 2006, Vancouver, Canada.

Tasaka, K. et al, 1990. "JNDC Nuclear Data Library of Fission Products [Second Version]", JAERI-1320, Japan Atomic Energy Institute.